An Initialization Scheme of Hurricane Models by Vortex Specification

YOSHIO KURIHARA, MORRIS A. BENDER, AND REBECCA J. ROSS

Geophysical Fluid Dynamics Laboratory, National Oceanic and Atmospheric Administration, Princeton University, Princeton, New Jersey

(Manuscript received 17 July 1992, in final form 23 November 1992)

ABSTRACT

A scheme is presented to improve the representation of a tropical cyclone in the initial condition of a high-resolution hurricane model. In the proposed method, a crudely resolved tropical cyclone in the large-scale analysis is replaced by a vortex that is properly specified for use in the prediction model.

Appropriate filters are used to remove the vortex from the large-scale analysis so that a smooth environmental field remains. The new specified bogus vortex takes the form of a deviation from this environmental field so that it can be easily merged with the latter field at the correct position. The specified vortex consists of both axisymmetric and asymmetric components. The symmetric component is generated by the time integration of an axisymmetric version of the hurricane prediction model. This ensures dynamical and thermodynamical consistency in the vortex structure, including the moisture field, and also compatibility of the vortex with the resolution and physics of the hurricane model. In the course of the integration of the axisymmetric model, the tangential wind component is gradually forced to a target wind profile determined from observational information and empirical knowledge. This makes the symmetric vortex a good approximation to the corresponding real tropical cyclone. The symmetric flow thus produced is used to generate an asymmetric wind field by the time integration of a simplified barotropic vorticity equation, including the beta effect. The asymmetric wind field, which can make a significant contribution to the vortex motion, is then added to the symmetric flow. After merging the specified vortex with the environmental flow, the mass field is diagnosed from the divergence equation with an appropriately controlled time tendency. The wind field remains unchanged at this step of initialization.

Since the vortex specified by the proposed method is well adapted to the hurricane prediction model, problems of initial adjustment and false spinup of the model vortex, a long-standing difficulty in the dynamical prediction of tropical cyclones, are alleviated. It is anticipated that the improvement of the initial conditions can reduce the error in hurricane track forecasting and extend the feasibility of tropical cyclone forecasting to intensity change.

1. Introduction

Results of experimental predictions using the multiply nested movable mesh (MMM) hurricane model of the Geophysical Fluid Dynamics Laboratory (GFDL) are encouraging regarding forecast capability, when combined with the National Meteorological Center (NMC) T80 global analyses. The model could simulate the accelerated movement of Hurricane Gloria (1985) as well as many of its observed structural features, including the strongly asymmetric distributions of the low-level wind and precipitation (Kurihara et al. 1990). On the other hand, the mismatch between the fine resolution of the hurricane model and the coarse resolution of the analysis, as well as physics differences between the hurricane model and the NMC model, caused a significant period of vortex adjustment after beginning the above-mentioned experimental predictions. Evidently, the NMC analyzed initial vortices, which were too large and too weak, underwent false spinup in the course of the model integration, especially during the first day or two of the forecast. Due to the slow spinup of the initial vortices, forecasting the storm intensity was out of the question, and predicted storm movement was often erratic in the early period of model integration. In one case, for example, the movement of the surface pressure minimum was strongly influenced by the low-level strong convergence that formed far north of the storm center during the vortex adjustment period. Apparently, this caused a deviation of the forecasted storm track from the observed track.

It is clear that resolving the problem of false spinup of the vortex will improve the skill of dynamical prediction of tropical cyclones. One solution is to make the initial model vortex more realistic, although this depends on the availability of often scarce observational data. The idea of improving the tropical cyclone representation with an empirical realistic vortex, often called a bogus vortex, is not new. Recent examples have included the works of Iwasaki et al. (1987) and Mathur (1991). An important and still unsolved issue in such an approach is that of vortex consistency with

Corresponding author address: Dr. Yoshio Kurihara, Geophysical Fluid Dynamics Laboratory, Princeton University, P.O. Box 308, Princeton, NJ 08542-0308.

the properties of the prediction model. Above all, the initial moisture field, which affects the intensity change of the vortex, has been especially difficult to specify in a realistic yet model-consistent manner. In the scheme presented here, model consistency is ensured by generating the symmetric component of the vortex with an axisymmetric version of the full hurricane prediction model. The obtained vortex is constrained so that it is realistic through the incorporation of observational information in the process of vortex generation. At present, the routinely acquired tropical cyclone observations are adaptable to a specification of the symmetric structure of a vortex but are insufficient to describe the asymmetric structure (Reeder et al. 1991). Nevertheless, with recognition of a possible contribution of the asymmetric structure to the vortex motion (e.g., Smith et al. 1990; Carr and Elsberry 1990), an attempt has recently been made to specify a model vortex that includes an asymmetric circulation obtained from an analytical model (Carr and Elsberry 1992). In another scheme, an empirically determined dipole circulation is imposed over the vortex area in order to control the vortex motion (Mathur 1991). Among the many factors that can influence the development of asymmetric structure in hurricanes, perhaps the simplest cause is the planetary vorticity advection by the symmetric flow within the vortex. Theoretical considerations (e.g., Ross and Kurihara 1992) indicate that the structure of the asymmetry induced by this mechanism strongly depends on the symmetric structure of the vortex. Therefore, in the present scheme, the former is generated from the symmetric vortex component obtained in the preceding step.

The specification of the improved vortex is just one aspect of this scheme of hurricane model initialization. The purpose of the present paper is to describe a comprehensive initialization scheme that removes the poorly resolved unrealistic vortex from the large-scale analysis, systematically generates a vortex possessing a realistic yet dynamically consistent structure, and smoothly incorporates the specified vortex into the large-scale field. It should be stressed that the generated vortex, which will also be referred to as a specified vortex, is compatible with the physics and grid resolution of the prediction model. In a companion paper (Bender et al. 1993), the improvements in predictions of vortex track and intensity due to the present initialization scheme will be reported. The proposed scheme will be useful until observations and analysis techniques of high-resolution three-dimensional data (e.g., Lord and Franklin 1987), or methods of data assimilation on the vortex scale, become operationally applicable.

The guidelines used in the formulation of the present initialization scheme are presented in section 2. The basic framework and methodology of the scheme that was constructed following these guidelines are described in sections 3–5. In particular, the topic of section 3 is the removal of the vortex from the large-scale analysis. In section 4, the systematic procedure used to generate model vortices is described. Section 5 deals with the problems of vortex merging and recomputation of mass fields. Section 6 describes in detail the empirical formulas and rules that were devised for the automated implementation of the proposed scheme. Some results of the automated implementation are presented in section 7. A few remarks regarding the initialization method are made in section 8.

2. Guidelines

Initial meteorological data for the MMM hurricane model grids are first transferred from the NMC global analysis through an appropriate interpolation method. The grid resolutions of the triply nested model telescopically increase from 1° to 1/3° and to 1/6° longitude–latitude. The finest resolution used can describe many of the features of a tropical cyclone vortex. As compared with the above resolution, the resolution of the transform grid of the global T80 spectral analysis is about 1.5° and is too coarse to resolve a realistic tropical cyclone structure. In the scheme proposed in this paper, a hurricanelike vortex, which will be referred to as the analyzed vortex, is removed from the global analysis and, instead, a specified vortex, which is model compatible and realistic, is added. Schematically, the scheme can be expressed as

$$\text{(initial field)} = \text{(global analysis)} - \text{(analyzed vortex)} + \text{(specified vortex)}.$$

In the present study, the analyzed vortex is defined as a deviation from the environmental field. Namely, the total field in the vicinity of the tropical cyclone is considered as a combination of an environmental field component and a deviation representing the analyzed vortex, while far from the tropical cyclone it is entirely the environmental field. The environmental field will be defined to smoothly change from the tropical cyclone area to the surrounding region. The size or the radius of the analyzed vortex, r_0, should be determined from aspects of the vortex in the analyzed field. The definition of the analyzed vortex as a deviation from the environmental field allows the removal of an inaccurately positioned vortex as a distinct and separate step from the later addition of a specified vortex at the observed location. In the extreme case in which the vortex is absent in the global analysis, r_0 is zero; the global analysis is equal to the environmental field and the specified vortex is added at the proper position.

To improve the representation of the tropical cyclone, three conditions are imposed on the vortex specification. First, the structure of the vortex should be dynamically and thermodynamically consistent. In addition to the relationship between the wind and mass fields, coherency of the moisture field to other variables is particularly important because the amount of dia-

batic heating, which affects the temperature tendency and, hence, the intensity change, is sensitive to the amount of moisture and convergence of the wind. Second, some major features of the real tropical cyclone should be present in the corresponding specified vortex. Real storms evolve in different environmental conditions and possess unique size and intensity characteristics. For example, the radius of the specified vortex, r_b, should be determined from the available information on the structure of the real hurricane. Third, the specified vortex has to be compatible with the resolution and physics of the prediction model. This condition is designed to prevent false spinup of the specified vortex. In the proposed scheme, the specified vortex also includes an asymmetric wind component that may significantly contribute to the movement of the vortex. The axisymmetric and asymmetric flows in the specified vortex should be dynamically consistent with each other.

The specified vortex is defined as a deviation from the environmental field. This facilitates inclusion of the specified vortex in the initial condition of the hurricane model; namely, the specified vortex can be simply added to the environmental fields at the appropriate location. Ease in repositioning the tropical cyclone is advantageous because the storm position in the large-scale analyses can be in error even by hundreds of kilometers.

The subtraction of an analyzed vortex and the addition of a specified vortex can introduce high-frequency motion in the prediction model integration due to imbalances between the wind and mass fields. Even if the environmental fields and the specified vortex are each separately balanced, high-frequency modes may appear in the combined fields because of the nonlinearity of the governing equations. Thus, in principle, a readjustment of the fields is needed for the model integration to start without significant imbalances. A condition used in this step is that the wind field should not be modified by the readjustment procedure. This is important because the wind field directly affects the vortex movement. Adherence to the above condition enables the observational influence incorporated in the generation of the wind field to be preserved.

In the following three sections, the basic framework of an initialization method that satisfies the above guidelines is described. Practical, specific details relating to the automated implementation of the scheme are given in section 6. A table of symbols used in this paper and their definitions is included in appendix A.

3. Removal of an analyzed vortex

The first phase of the present initialization procedure is the removal of a poorly resolved tropical cyclone from the given large-scale analysis. Admittedly, there is no unique method for defining a tropical cyclone system in the analyzed field in which it exists. The guideline set forth in the preceding section concerning the field separation is that the field remaining after the removal of the analyzed vortex should vary smoothly across the region of the removed vortex.

In the present scheme, an original scalar field h, such as the surface pressure, zonal and meridional components of wind, temperature, or mixing ratio of water vapor, is first split into the basic field h_B and the disturbance field h_D by using a filtering operator:

$$h = h_B + h_D. \tag{3.1}$$

The basic field represents the large-scale general features in the analysis, while the disturbance field is the deviation of h from the basic field. Next, the analyzed vortex is isolated and removed from the disturbance field with the use of a cylindrical filter. The size of an analyzed vortex h_{av}, which is appropriately determined for each case, defines the filter radius. The environmental field, h_E, is then defined by recombining the remaining nonhurricane disturbance field with the basic field:

$$h_E = h_B + (h_D - h_{av}). \tag{3.2}$$

It is obvious that the environmental field thus obtained is identical to the original large-scale analysis, except within the cylindrical filter radius where the analyzed vortex is missing:

$$h_E = h - h_{av}. \tag{3.3}$$

The above-mentioned separation process is shown schematically in Fig. 1 for an idealized vortex superposed on a large-scale Haurwitz wave (Bender and Kurihara 1987). The radial extent of the cylindrical filter, r_0, is shown in the panel. Comparison of the initial field h with the two final components, h_E and h_{av}, indicates that the two-step filtering process successfully separated the vortex from the environment. The large-scale variation in the initial analysis h is slightly damped in the basic field h_B, but it is restored in the environmental field h_E by including the nonhurricane deviation, $h_D - h_{av}$.

The filtering operator that is iteratively applied in the decomposition (3.1) is a local three-point smoothing operator of the same form as that of Kurihara et al. (1990). Smoothing is first carried out in the zonal direction as follows:

$$\bar{h}_{\lambda,\varphi} = h_{\lambda,\varphi} + K(h_{\lambda-1,\varphi} + h_{\lambda+1,\varphi} - 2h_{\lambda,\varphi}). \tag{3.4}$$

In (3.4), h is the variable being smoothed, $\bar{h}$ is the zonally smoothed value, and the subscripts λ and φ, respectively, refer to the longitude and latitude (in degrees; $\lambda + 1$ and $\lambda - 1$ being the longitudes differing from λ by a distance of 1°). The coefficient K is the filtering parameter defined by

$$K = \frac{1}{2}\left(1 - \cos\frac{2\pi}{m}\right)^{-1}. \tag{3.5}$$

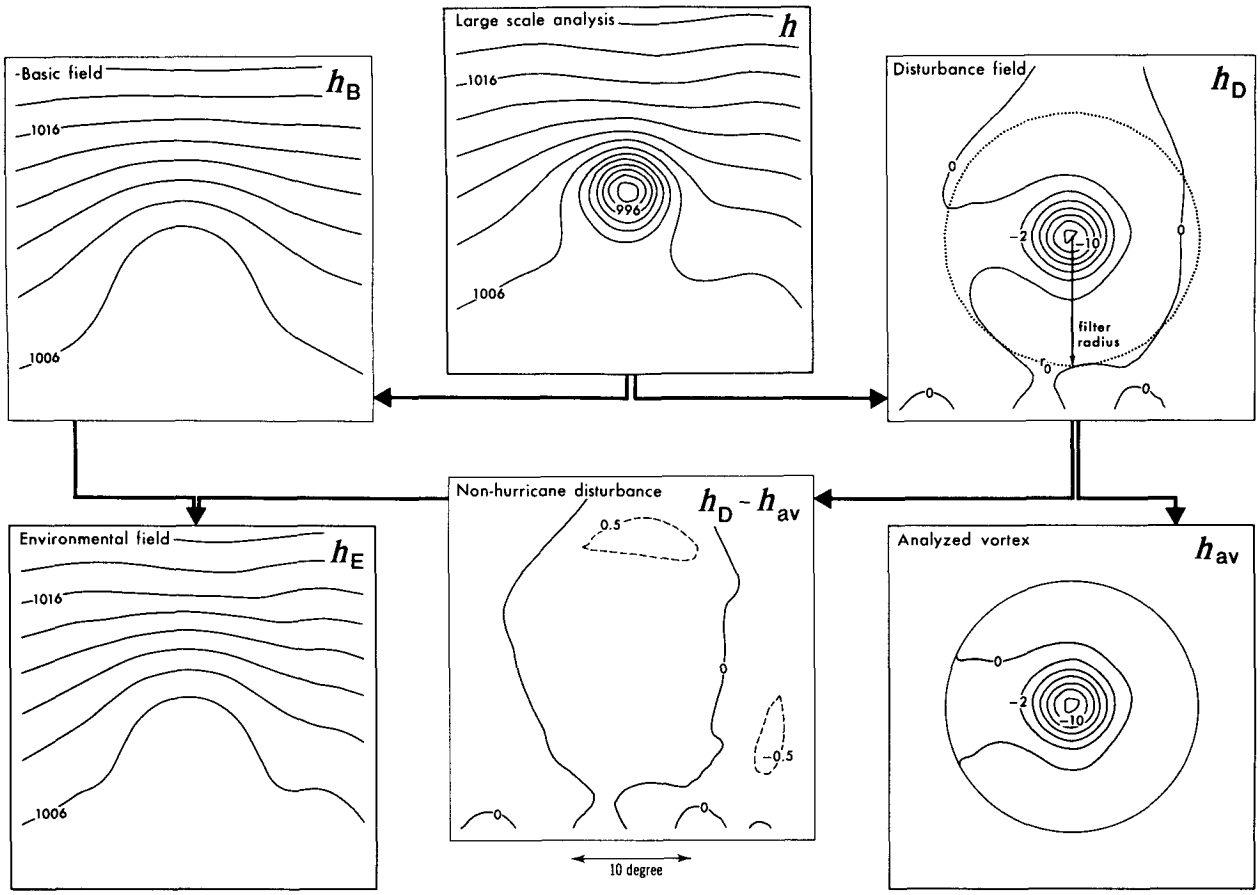

FIG. 1. Schematic diagram showing the separation of the large-scale analysis h into the environmental field h_E and the analyzed vortex h_{av}. The field h_E is defined to consist of the spatially filtered large-scale basic state h_B and a nonhurricane disturbance field $h_D - h_{av}$. In practice, the latter field may have more variability than this example beyond the filtering radius r_0.

In the course of successive applications of (3.4), m in (3.5) sequentially varies as 2, 3, 4, 2, 5, 6, 7, 2, 8, 9, 2. Values at the east and west endpoints are kept unchanged during the iteration. After the completion of smoothing in the zonal direction, h_B is obtained by a similar smoothing of the $\bar{h}$ field in the meridional direction, with iterative use of the following operator:

$$h_{B\lambda,\varphi} = \bar{h}_{\lambda,\varphi} + K(\bar{h}_{\lambda,\varphi-1} + \bar{h}_{\lambda,\varphi+1} - 2\bar{h}_{\lambda,\varphi}). \quad (3.6)$$

If the above filtering operator is applied to a field of sinusoidal waves, components with less than 9° wavelength will be completely filtered and the amplitudes of those with 15°, 20°, and 30° wavelength will be reduced by 82%, 60%, and 32%, respectively, as illustrated in Fig. 2a. The amplitude of the Haurwitz wave shown in Fig. 1 is reduced by 68% through this filtering. Thus, there is no sharp scale cutoff in the resulting basic field. By definition, the difference between the original value h and h_B is h_D.

The isolation of an analyzed hurricane vortex h_{av} from the disturbance field h_D is accomplished with the following cylindrical filter centered at the location of the analyzed tropical cyclone:

$$h_{av}(r, \theta) = h_D(r, \theta) - \{h_D(r_0, \theta)E(r) + \overline{h_D}(r_0)[1 - E(r)]\}, \quad (3.7)$$

where the polar coordinate system (r, θ) is used, and r_0 represents the radius of the filtering domain. The determination of the center position of the analyzed tropical cyclone and the filter radius is described in section 6a. The function $E(r)$, for $0 \leq r \leq r_0$, in (3.7), determines the filtering characteristics. It is required that $E(r)$ smoothly change with radius from the interior to r_0 and that h_{av} gradually diminishes to zero at the filter edge. As seen from (3.3), this guarantees the smoothness of the environmental field across the r_0 boundary. The empirically determined functional form of the factor $E(r)$ is

$$E(r) = \frac{\exp[-(r_0 - r)^2/l^2] - \exp[-(r_0)^2/l^2]}{1 - \exp[-(r_0)^2/l^2]}, \quad (3.8)$$

where l is a parameter controlling the filtering shape and, in the present study, is set to 1/5 of r_0. The radial profile of $E(r)$ is shown in Fig. 2b. Since $E(r)$ is unity at $r = r_0$, h_{av} does not exist at the radius r_0. Also, h_{av} is set to zero beyond this radius. Note that within the radius $r_0 - l$, the disturbance field h_D is comprised mostly of the analyzed vortex field h_{av} (see Fig. 1). The overbar in (3.7) indicates an average along the periphery of the filter, that is, at the radius r_0:

$$\overline{h_D}(r_0) = \frac{1}{2\pi} \oint h_D(r_0, \theta) d\theta. \qquad (3.9)$$

This represents an estimate of the nonhurricane disturbance field at the center position of the analyzed vortex and guarantees smooth variation of the nonhurricane disturbances across the storm center. In practice, the magnitude of (3.9) has been very small as compared with that of h_D.

4. Specification of a model vortex

The vortex that replaces the analyzed hurricane should possess the three properties mentioned in section 2: structural consistency, resemblance to the corresponding real storm, and compatibility with the hurricane prediction model. Such a vortex can be generated from the time integration of the hurricane model with an observationally derived constraint imposed on the wind field. In the scheme described below, an axially symmetric component of the vortex is first generated, and an asymmetric component is derived from it.

a. Axisymmetric component

An axisymmetric version of the GFDL hurricane model used by Kurihara et al. (1990), expressed in the r (radial distance) – σ (pressure normalized by the surface value) coordinate system, is time integrated to create the symmetric part of the vortex. By doing so, the generated vortex is compatible with the prediction model configuration, including the horizontal and vertical grid resolution and computational schemes, as well as with the model physics. Also, the symmetric fields of wind, mass, and moisture that evolve in the course of the vortex generation are mutually consistent. Thus, it is anticipated that fictitious spinup of the model hurricane after the start of dynamical prediction with the full three-dimensional model will be substantially reduced or even eliminated.

In order to make the generated vortex realistic, an appropriate target state is prescribed toward which the symmetric vortex wind field is forced during the time integration of the axisymmetric model. The target state, in which available observational data are incorporated, represents the best estimate of the tangential wind profile of the particular real tropical cyclone. The general procedure to estimate the target tangential wind profile requires the determination of a "first-guess" profile.

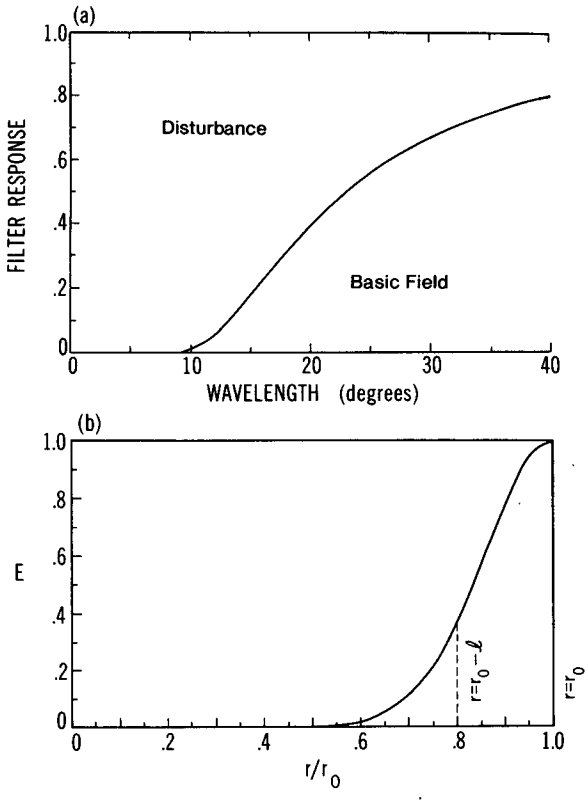

FIG. 2. (a) Response to the filter used to separate a field into the basic field and the disturbance. The result from the application to a field of sinusoidal waves is shown. (b) Radial profile of the filtering function $E(r)$ used in (3.7). It describes the ratio of the nonhurricane disturbance at the radius r to that at r_0 (with a nonhurricane disturbance at the center subtracted from each disturbance) as a function of radius. Vertical lines indicate the radial distance corresponding to the filter radius r_0 and the radius $r_0 - l$, where $l = 0.2r_0$, within which filtering is strong.

This profile can be based on empirical formulas reflecting our general understanding of the tropical cyclone structure. The available wind observations are then used to modify the "first-guess" profile in order to incorporate the structural characteristics of each individual tropical cyclone. Note that the first-guess profile must be reasonably accurate because its influence on the target wind profile can be large. Also, since the target profile is defined as a wind deviation from the environmental flow, the latter must be correctly excluded from each observation. The above processing is performed separately for four quadrants: northeast, northwest, southwest, and southeast. The resulting four modified profiles are then averaged to define the target tangential wind.

Under ideal conditions, a sufficient number of wind observations would be available in a large space surrounding the storm. Thus far, in practice, however, the availability of observational data and information has been limited mostly to low levels. Accordingly, in the present simplified scheme, the target tangential wind

is determined by the above method only at the model level near the top of the planetary boundary layer. Its radial profile $\langle V_d$ is used to obtain the target tangential winds in the free atmosphere $\langle V\rangle$ through $F(\sigma)$, a functional representation of the vertical profile of the tangential wind:

$$\langle V\rangle(r, \sigma) = F(\sigma)\langle V_d\rangle(r). \quad (4.1)$$

The target winds are not needed within the planetary boundary layer because a model-compatible boundary-layer structure will evolve during the axisymmetric model integration. The specific details of the determination of the first-guess profile, and the techniques used to process and incorporate observational information, are presented in section 6b. In situations where the observational data coverage is more extensive, the above procedure of data incorporation can be altered. Some considerations regarding this issue are discussed in appendix B.

The present scheme requires the specification of the radial extent of the symmetric vortex, r_b. The target wind profile is defined to vanish at this radius. In the present scheme, the radius r_b is specified as twice the radius of the outermost closed isobar (at the surface), a subjectively determined parameter available from forecast centers. The latter radius, r_{out}, which may be found in the NMC tropical cyclone information message or assigned a value otherwise, is sometimes used as a measure of the size of a tropical cyclone. However, the average tangential wind is usually not negligibly small at this radius but extends considerably beyond.

The time integration of the axisymmetric model begins from a state of rest, that is, u (radial wind) = 0, and v (tangential wind) = 0. The initial temperature and moisture fields are radially uniform, with vertical stratifications equivalent to the respective basic fields at the observed hurricane position. The surface pressure is also radially uniform initially and is set to the basic-field value at the observed center. During generation of the symmetric vortex, the tangential wind is predicted and modified after each time step so that it gradually approaches the target wind. However, no constraint is imposed on the evolution of the radial wind, temperature, moisture, and surface pressure.

The usage of two time scales is a unique feature in the present scheme of tangential wind forcing. Namely, a long time scale is used to determine a time-dependent reference wind from the target wind profile. The model-predicted wind is then relaxed toward this reference wind, with a short time scale after each integration time step. Specifically, the reference wind V_R is defined so that it slowly increases with time from zero at the initial time to the target wind value at the end of the long time scale (a period assumed for gradual forced development of a vortex) τ, which is set to 60 h:

$$V_R = \langle V\rangle \exp\left(1 - \frac{\tau}{t}\right). \quad (4.2)$$

The model-predicted tangential wind v is replaced after each time step with the forced value v_F defined as

$$v_F = \frac{V_R + \alpha v}{1 + \alpha}, \quad (4.3)$$

where the weighting parameter α is related to the relaxation time, that is, the short time scale. A small α implies a strong forcing. See section 6c for specific details about the time integration, including the surface boundary conditions, the length of the axisymmetric model integration, and the values of the parameter α. As previously mentioned, no forcing is applied to the tangential wind in the planetary boundary layer, enabling model-consistent winds to freely develop there. With this forcing technique, the model vortex gradually evolves towards a realistic state through a succession of nearly balanced states.

The symmetric flow of the specified vortex is set to the winds generated in the axisymmetric model. On the other hand, the temperature, moisture, and surface pressure of the specified vortex are defined as the deviations of these fields in the generated vortex from the respective conditions at the vortex periphery, that is, at the radius r_b.

b. *Asymmetric component*

As mentioned in section 1, asymmetric winds induced by the effect of planetary vorticity advection within a symmetric vortex can play a significant role in the motion of the vortex. In the present scheme, an asymmetric flow is generated from the symmetric flow component and included in the initial condition of the model. This ensures consistency between the symmetric and asymmetric flows and incorporates the influence of the asymmetric flow from the start of the hurricane prediction. If no asymmetry is present in the initial condition, a long time (1–2 days) is required before the vortex exhibits quasi-steady propagation due to the above beta effect.

Vorticity asymmetry is generated by a simple scheme formulated by Ross and Kurihara (1992) on the basis of the barotropic vorticity equation. In their scheme, the vorticity field, which is expressed in the polar coordinate system (r, θ), is projected onto azimuthal wavenumber space and truncated after wavenumber two. Hence, the vorticity field is expressed by

$$\zeta(r, \theta) = \zeta_0(r) + \zeta_1(r, \theta) + \zeta_2(r, \theta), \quad (4.4)$$

where the subscript denotes the azimuthal wavenumber, with the wavenumber zero referring to the symmetric vortex. Correspondingly, the wind vector $\mathbf{V}$ (in the inertial frame) is also decomposed:

$$\mathbf{V}(r, \theta) = \mathbf{V}_0(r) + \mathbf{V}_1(r, \theta) + \mathbf{V}_2(r, \theta). \quad (4.5)$$

The governing equations for the vorticity components on a beta plane, in the coordinate system moving with the velocity $\mathbf{C}$, are

$$\frac{\partial \zeta_0}{\partial t} = -(\mathbf{V}_1 \cdot \nabla \zeta_1)_0 - (\mathbf{V}_2 \cdot \nabla \zeta_2)_0 + (\mathbf{C} \cdot \nabla \zeta_1)_0 - \beta(\mathbf{j} \cdot \mathbf{V}_1)_0 \quad (4.6)$$

$$\frac{\partial \zeta_1}{\partial t} = -\mathbf{V}_0 \cdot \nabla \zeta_1 - \mathbf{V}_1 \cdot \nabla \zeta_0 - (\mathbf{V}_1 \cdot \nabla \zeta_2)_1 - (\mathbf{V}_2 \cdot \nabla \zeta_1)_1 + \mathbf{C} \cdot \nabla \zeta_0 + (\mathbf{C} \cdot \nabla \zeta_2)_1 - \beta \mathbf{j} \cdot \mathbf{V}_0 - \beta(\mathbf{j} \cdot \mathbf{V}_2)_1 \quad (4.7)$$

$$\frac{\partial \zeta_2}{\partial t} = -\mathbf{V}_0 \cdot \nabla \zeta_2 - \mathbf{V}_2 \cdot \nabla \zeta_0 - (\mathbf{V}_1 \cdot \nabla \zeta_1)_2 + (\mathbf{C} \cdot \nabla \zeta_1)_2 - \beta(\mathbf{j} \cdot \mathbf{V}_1)_2, \quad (4.8)$$

where $(\mathbf{A} \cdot \mathbf{B})_n$ is the wavenumber n component that results from the inner product of two vectors **A** and **B**, and **j** is the unit vector pointing to the north. The velocity **C** is the wind velocity at the vortex center solely due to the generated vorticity asymmetry; it depends only on ζ_1. Note that the vectors **C** and **j** are, respectively, wavenumber one quantities in the polar coordinate expression.

Numerical integration of (4.6), (4.7), and (4.8) is carried out by radially dividing each vorticity component field into vortex rings, with width equivalent to the horizontal resolution of the hurricane prediction model, and estimating the radial derivative by finite differencing. The field of each velocity component can be easily obtained from the vorticity field of the corresponding component. In the present scheme, the asymmetric wind is obtained first for the boundary-layer top. Accordingly, the initial condition for the time integration is taken from the symmetric tangential wind at the boundary-layer top, generated previously by the axisymmetric model integration, with very small-scale radial variation removed by weak local smoothing. In order to obtain an accurate solution to the vorticity equation, the integration domain should be much larger than the size of the initial symmetric vortex because asymmetric flow will generally be induced well beyond the extent of the initial vortex. In the present scheme, the asymmetric flow is computed for the entire MMM model domain. As discussed by Ross and Kurihara (1992, section 4), however, the far-field asymmetry developed in the present simple model will be affected by inaccuracies in the symmetric profile and actually can be too strong for cases of very large, strong vortices, causing unfavorable influence on the prediction. Furthermore, it may be expected that the vorticity field far from the vortex is well represented by the global analysis. To alleviate the problem of far-field vorticity generation, the same form of Newtonian damping as described in their paper is applied to the equations for the asymmetric vorticity components. The parameters are set such that no damping occurs from the vortex center out to the radius $r_b/1.9$, and the damping increases from this radius outward, with a damping time of 12 h specified at the radius r_b. The length of the time integration of the truncated vorticity equation is a subjective parameter that can influence the resultant asymmetric field. An empirical approach relating this parameter to observed changes in the storm intensity is discussed in section 6d.

The generated asymmetric wind is applied at the top of the planetary boundary layer. At upper levels, the asymmetric component is decreased by the same factor describing the vertical profile of the target tangential wind, that is, $F(\sigma)$ of (4.1).

5. Diagnosis of the mass field

a. Implantation of the specified vortex

The specified tropical cyclone generated in the previous section consists of two parts: 1) the mutually consistent symmetric fields (deviations from the environment) of wind, mass, and moisture within the radius r_b, and 2) the asymmetric wind, including a very small change in the symmetric flow due to (4.6), over the entire model domain. Both parts are centered at the correct hurricane location on the model domain and are merged with the environmental fields, that is, h_E in (3.3). Because the specified vortex is defined as a deviation from the environment in analogous fashion to (3.3), the merging is simply performed by addition. If part of the symmetric vortex is located over land, the water vapor mixing ratio deviation is reduced by 50% at the land grid points before being added onto the environmental field because the symmetric vortex is generated with an ocean surface condition.

The resulting fields of wind and moisture are ready for use as initial conditions. However, those of the surface pressure and temperature (or the geopotential), which will be denoted, respectively, by p_*^0 and T^0 (or ϕ^0), can no longer be regarded as precisely balanced with the wind field because of the nonlinearity of the relation between the wind and mass field. In addition, the asymmetry obtained in the preceding section is for the wind field only. In principle, it is reasonable to readjust the fields to a state of balance; a scheme to perform it is described below. Preliminary studies for some cases indicate that, in practice, the recomputation of the mass field in these cases could be skipped without deteriorating the prediction. This suggests that the environmental field and the generated vortex were, respectively, in a state of highly accurate balance and the implantation of the generated vortex did not cause a problem.

b. Diagnosis of the mass field

Following the guideline stated in section 2, the wind field obtained above has to remain unchanged at this final phase of initialization. This is ensured by the use of a static initialization method, in which the unknown mass fields p_* and T (or the geopotential ϕ) are deter-

mined for a known wind field V. Specifically, the diagnostic tool used is the divergence equation with the frictional effect included and the time-tendency term controlled by the slow-moving advection mode defined below. The occurrence of an excessive divergence tendency at the initial time can be avoided by this method. Although there is no guarantee that a large time tendency will not occur in the temperature field at the initial time, the consistency of the moisture field (a source of diabatic effects) with the wind field may reduce this possibility. In the present scheme, consistency between these two fields exists in the symmetric component of the specified vortex. The consistency is degraded by the absence of asymmetry in the moisture field as well as by merging of the specified vortex with the environmental field. However, the experimental predictions performed thus far have shown no apparent sign of problem, indicating that the above residual inconsistency did not lead to vortex spinup.

In this subsection, the subscripts d and a will be used to indicate quantities at the boundary-layer top ($\sigma = \sigma_d$) and those of the atmospheric surface layer, respectively. Also, the subscripts B and D have the same meaning with those expressed in (3.1), that is, the basic and disturbance fields, respectively. The brackets [ ] indicate the deep-layer mean of the quantity, vertically integrated over the entire σ range. As defined in section 5a, the fields obtained by implanting the specified vortex to the environmental field are denoted by the superscript 0.

The divergence equation in the σ-coordinate system takes the following form:

$$G = \nabla^2\phi + \nabla\cdot(RT\nabla \ln p_*), \tag{5.1}$$

where R is the gas constant, and the quantity G is obtained from the momentum distribution. The right-hand side is derived from the momentum equation in which the pressure gradient force is split into two terms to facilitate the diagnosis of both p_* and T. The mass-dependent right-hand side of (5.1) will be determined so as to balance with G. The form of G is

$$G = -\frac{\partial D}{\partial t} + \nabla\cdot\left\{-(\mathbf{V}\cdot\nabla)\mathbf{V} - \dot{\sigma}\frac{\partial \mathbf{V}}{\partial \sigma} - \left(f + \frac{\tan\varphi}{a}u\right)(\mathbf{k}\times\mathbf{V}) + \mathcal{F}\right\}, \tag{5.2}$$

where D is the divergence, u is the zonal component of the wind $\mathbf{V}$, f is the Coriolis parameter, φ is the latitude, a is the radius of the earth, $\mathbf{k}$ is the vertical unit vector, and $\mathcal{F}$ represents the frictional force. As indicated by Neumann (1979), the motion of hurricanes may be approximated by the deep-layer mean of the large-scale flow. This idea is used to approximate the local divergence tendency as

$$\frac{\partial D}{\partial t} \approx \frac{\partial D_D}{\partial t} \approx -[\mathbf{V}_B]\cdot\nabla D_D, \tag{5.3}$$

where $[\mathbf{V}_B]$ represents the deep-layer mean of the large-scale basic flow. Thus, the magnitude of the divergence tendency is controlled by a slow propagation speed. The other terms in G are estimated by the same scheme with those used in the MMM model.

Diagnostic formulas for the surface pressure and geopotential are derivable from (5.1). In this study, however, (5.1) is not used for the boundary layer but applied only for the free atmosphere because an accurate diagnosis of ϕ in the boundary layer is difficult due to the complicated dynamical balance involving large frictional effects. The initial temperature in the boundary layer is estimated simply by setting $T = T^0$. Applying (5.1) to the level σ_d, and substituting ϕ_d^0 and T_d^0 for ϕ and T on the right-hand side, the equation for p_* is obtained:

$$\nabla\cdot(RT_d^0\nabla \ln p_*) = G_d - \nabla^2\phi_d^0. \tag{5.4}$$

In the computation of G_d, the vertical σ velocity at the σ_d level is approximated by the vertical integral of $\nabla\cdot\mathbf{V}$ with respect to σ from σ_d to 1. Once p_* is known, the geopotential can easily be computed from (5.1), written as

$$\nabla^2\phi = G - \nabla\cdot(RT^0\nabla \ln p_*). \tag{5.5}$$

When (5.4) and (5.5) are applied to a dataset with steep topographic gradients, accuracy problems can arise from the large variation of p_*. This difficulty was avoided by the use of $\phi - \phi_*$, where ϕ_* is the geopotential of the bottom surface ($\sigma = 1$) and the sea level pressure p_s in the mass diagnosis formulas as rewritten below. Gradients of these variables are smooth regardless of the ruggedness of topography.

In the present scheme, the surface pressure and the sea level pressure at a station are related by

$$p_* = p_s\left\{1 + \frac{\Gamma\phi_*}{gT_a}\right\}^{-g/R\Gamma}, \tag{5.6}$$

where Γ is the mean atmospheric lapse rate ($\sim$6.7 K km^{-1}), and g is the acceleration of gravity. In practice, the temperature at the lowest model level is taken for T_a using the following approximations:

$$\ln p_* \approx \ln p_s - \frac{\phi_*}{RT_a} \tag{5.7}$$

and

$$\nabla T_a \approx -\left(\frac{\Gamma}{g}\right)\nabla\phi_*. \tag{5.8}$$

The following conversion formula is obtained from (5.6):

$$\nabla \ln p_* = \nabla \ln p_s - \frac{1}{RT_a}\left\{1 + \frac{\Gamma\phi_*}{gT_a}\right\}\nabla\phi_*. \tag{5.9}$$

The diagnostic formulas (5.4) and (5.5) are rewritten, after manipulations,

$$\nabla\cdot(RT_d^0\nabla \ln p_s) = G_d - \nabla^2(\phi_d^0 - \phi_*) + \nabla\cdot\{(H_d - 1)\nabla\phi_*\}, \quad (5.10)$$

and

$$\nabla^2(\phi - \phi_*) = G - \nabla\cdot\{RT^0\nabla \ln p_s - (H - 1)\nabla\phi_*\}, \quad (5.11)$$

where

$$H = \frac{T^0}{T_a^0}\left\{1 + \frac{\Gamma\phi_*}{gT_a^0}\right\}. \quad (5.12)$$

The quantity H is generally close to one, and the gradient of $\phi_d^0 - \phi_*$ is very small. Thus, solutions of (5.10) and (5.11), respectively, tend to be smooth.

In practice, by replacing T_d^0 in (5.10) with its basic field component, $(T_d^0)_B$, and assuming that the gradient of the latter is negligible, the left-hand side of (5.10) can be simplified to the form $R(T_d^0)_B\nabla^2 \ln p_s$. A relaxation method may be used to obtain $\ln p_s$ as well as $(\phi - \phi_*)$ for appropriate boundary conditions, for example, the Dirichlet condition determined from an available analysis. The solutions can easily be converted back to p_* and ϕ.

The temperatures in the free atmosphere are then computed from the vertical profile of ϕ through the hydrostatic relation

$$T = -\frac{1}{R}\frac{\partial\phi}{\partial \ln\sigma}. \quad (5.13)$$

Vertical interpolation of ϕ may be required in this calculation, depending on the finite-difference scheme used. In such cases, interpolation of the increment of ϕ, that is, the deviation from a certain reference profile by means of smooth curve fitting seems to yield a good result. After obtaining T, the mixing ratio of water vapor is checked and reduced to the saturation value, if it exceeded the latter.

A comment is added here concerning a minor correction for the divergent component of the wind that may be needed after the computation of the surface pressure through (5.10). The correction may be made in order to suppress the possible appearance of very large time changes at the initial time in the tendency equation:

$$\frac{\partial p_*}{\partial t} = -[\nabla\cdot(p_*\mathbf{V})]. \quad (5.14)$$

To bound the pressure tendency, a condition similar to (5.3) is used,

$$\frac{\partial p_*}{\partial t} \approx \frac{\partial p_{*D}}{\partial t} \approx -[\mathbf{V}_B]\cdot\nabla p_{*D}. \quad (5.15)$$

If a large difference exists between the right-hand sides of (5.14) and (5.15), the following equation, in which p_* is replaced by p_s to deal with the topography, is solved for χ,

$$\nabla^2\chi = -[\nabla\cdot(p_s\mathbf{V})] + [\mathbf{V}_B]\cdot\nabla p_{sD}. \quad (5.16)$$

The wind is modified by adding $c\nabla\chi$ to $p_s\mathbf{V}$, where c is a σ-dependent function whose vertical integral is unity. In the present scheme, the function c is such that the wind modification is uniformly distributed over the free atmosphere below the tropopause. To solve (5.16) numerically by a relaxation method, boundary conditions can be imposed at a certain distance outside of the model domain in order to reduce its influence on the solution. The wind correction does not affect the rotational flow, including the asymmetric wind computed in the previous section. The correction is not needed if the total divergence $[\nabla\cdot\mathbf{V}]$ is negligible. For the test cases examined so far, this correction step could be skipped without any problem. However, this step may be required if the availability of wind observations becomes more extensive, as assumed in appendix B, and the method of vortex specification is modified.

6. Automated implementation of the proposed scheme

The implementation of the present initialization scheme necessarily involves the determination of numerical values such as the size of the analyzed vortex, the target wind field, the integration period for the vortex generation, and so on. Tests of this scheme with subjectively assigned parameter values have produced very satisfactory results, as reported in Bender et al. (1993).

Recently, in an effort to eliminate the need for subjective specification, and guided by these earlier tests, an automated procedure has now been developed for the determination of these factors. Ideally, an automated system in general should function over a broad range of conditions or for a variety of input datasets, while still producing end results of a reasonable accuracy in all cases. In the present automation, empirical formulas have been devised by which the observed storm information for a particular tropical cyclone is related to the functions and parameter values appropriate for that storm. Routine observations, special datasets, and available messages, such as the marine advisory reports, provide valuable data for the construction of a realistic tropical cyclone structure in the initial condition. The most important data source is the tropical cyclone message available every 6 h from NMC, which includes the following basic information: longitudinal and latitudinal position of the storm (λ_c, φ_c); central pressure p_c; pressure of the outermost closed isobar p_{out}; radius of the outermost closed isobar r_{out}; maximum surface wind speed $V_{\max}$; radius of maximum wind $R_{\max}$, radius of 15 m s^{-1} wind in each of the northeast, northwest, southeast, and southwest

quadrants; and storm-depth category—shallow, medium, and deep. Of the parameters in the above list, at least (λ_c, φ_c) through $R_{\max}$ are needed for the present automated scheme, and these quantities must be assigned a value either from a report or by an estimate. All of the formulas and rules presented in this section have worked quite well in the real data experiments performed so far. As more experiments are performed, however, some modification of the specifics may be necessary.

a. The filter to remove an analyzed vortex (referred to in section 3)

The cylindrical filter in (3.7) is used to isolate the analyzed tropical cyclone vortex from the disturbance field. The filter is placed to contain the analyzed vortex. The determination of the filter center position and radius is based on the assumption that the disturbance wind is strong in the storm region. Let V_D be the wind speed of the disturbance field at the boundary-layer top. In the case in which a tropical cyclone is weak or absent in the analysis, there is an option to omit the step to remove the analyzed vortex. The filter center, or equivalently, the center of the hurricane in the large-scale analysis, is identified using an 11° × 11° subdomain (121 points on a 1° grid) centered on the grid point nearest to the observed storm position (λ_c, φ_c). The location of the wind-speed centroid within this subdomain defines the position of the filter center, (λ_0, φ_0),

$$\lambda_0 = \frac{\sum V_{Di,j}\lambda_{i,j}\Delta S_{i,j}}{\sum V_{Di,j}\Delta S_{i,j}}, \quad \varphi_0 = \frac{\sum V_{Di,j}\varphi_{i,j}\Delta S_{i,j}}{\sum V_{Di,j}\Delta S_{i,j}}, \quad (6.1)$$

where i and j are the gridpoint indices, and $\Delta S_{i,j}$ is the area assigned to the grid point. Thus, there is a practical assumption that the analyzed vortex center lies within approximately 5.5° of the observed storm position.

The size of the filter is determined from the profile of $\bar{V}_D(r)$, which represents the circular mean of V_D at a radius r from the filter center. Experience indicates that beyond a radius larger than R_{DM}, the position of maximum V_D, the profile of $\bar{V}_D(r)$ tends to smoothly decrease with radius and eventually levels off to a relatively small value. Presumably, this value is primarily due to the nonhurricane component in the disturbance wind field and indicates that the vortex component is contained within a certain radius. To determine this distance, the condition $\bar{V}_D < 6$ m s^{-1} and $-\partial\bar{V}_D/\partial r < 4 \times 10^{-6}$ s^{-1} is tested outward from the radius $1.5R_{DM}$ for each radius at an increment of 0.1° length. The second time that this condition is met, that radius, r_f, is assumed to contain the major portion of the analyzed hurricane. If the test condition is not met before $\bar{V}_D$ decreases to 3 m s^{-1}, then that radius is used for r_f. Alternatively, if neither condition is met before r reaches 1200 km, r_f is set to this upper limit. Finally, to ensure that the filter radius completely encloses the hurricane vortex, the filter radius r_0 is defined as $1.25r_f$.

b. Target tangential wind (referred to in section 4a)

In the present simplified scheme, only low-level wind information is used in the determination of the target tangential wind profile. Specifically, the general procedure to obtain the target profile mentioned in section 4a is applied only to the level at the boundary-layer top. If the wind data at this level are available from observations, the deviations of their tangential components (relative to the observed storm center) from those of the environmental flow, at respective observation points, are computed and used to modify the first-guess profile. Additionally, any available information on the surface wind is also utilized in this step. In most cases tested thus far, the surface wind data have been the only reported information available. The surface wind values are multiplied by the factor 1.35, which was empirically obtained on the basis of numerical results from the MMM model, to approximate the magnitude of the tangential component of the wind at the boundary-layer top. An exception is the surface value of $V_{\max}$, which is multiplied by 1.1, and then reduced by a small value $\Delta V_{\max}$, which crudely represents the wind component due to the storm asymmetry. Note that the asymmetric flow is determined later and is incorporated into the specified vortex. Because the magnitude of the asymmetry is related to the intensity and size of the symmetric vortex, the reduction amount (in meters per second) is computed by

$$\Delta V_{\max} = 0.1 + \frac{1000 - p_c}{50} + \frac{r_b - 600}{400}, \quad (6.2)$$

where p_c is in hectopascals, and r_b, which is equal to $2r_{\text{out}}$, is in kilometers.

After the wind data are adjusted to the boundary-layer top, they are grouped in four quadrants as mentioned in section 4a. Within each quadrant, the azimuthal position of each observation is ignored, and only the radial distance from the storm center is retained. The data thus arranged in each quadrant will be denoted by V_{obs}. In most cases, wind observations are quite sparse at outer radii near r_b. Therefore, the observations in each quadrant are supplemented at ten equally spaced points for the radial range between the radial location of the outermost observation point r_a and the radius r_b in order to provide a reasonable constraint for the profile. A formula to compute winds at these radii is

$$V_{\text{obs}}(r) = V_{\text{obs}}(r_a)\left(\frac{r_a}{r}\right)^A\left(\frac{r_b - r}{r_b - r_a}\right)^B, \quad (6.3)$$

which produces a decreasing wind profile with increasing radius between r_a and r_b. With $A = 1$ and $B = 1$

in (6.3), the relative angular momentum linearly decreases with increasing radius. The rate of decrease beyond r_a is reduced by computing the factors A and B by

$$\begin{cases} A = 1, B = 1; \quad \text{for} \quad p_c \geq 990 \\ A = 1 - 0.008(990 - p_c), \\ B = 1 - 0.006(990 - p_c); \\ \qquad \text{for} \quad 990 > p_c > 940 \\ A = 0.6, B = 0.7; \quad \text{for} \quad p_c \leq 940, \end{cases} \tag{6.4}$$

where p_c is in units of hectopascals. The tangential wind is assumed to be zero at r_b and at the storm center.

The target wind profile is first obtained separately for each quadrant by modifying the first-guess profile to fit the data V_{obs}. It is clear that the determination of the first-guess profile is important since it can have a significant impact on the target tangential wind in the data-sparse region. In the present procedure, where the profile modification is performed only at the boundary-layer top, the first-guess profile is determined by empirical formulas based on known surface characteristics of the tropical cyclone. Specifically, within the radius R_{max}, a Rankine vortex, $\langle V_d \rangle r^{-1} =$ constant (Depperman 1947), is used, while beyond R_{max} the profile is determined from equation (4) of Holland (1980), which uses observed parameters $p_{out} - p_c$, V_{max}, R_{max}, and the latitude φ_c. The difference between each V_{obs} in each quadrant and the Holland profile is interpolated by the scheme proposed by Akima (1970) to determine the correction to the first-guess profile at any radius. The addition of this difference to the Holland profile yields the radial profile of the tangential wind for that quadrant. The profiles of the four quadrants are then averaged to finally define the target tangential wind profile $\langle V_d \rangle$ at the boundary-layer top.

The vertical structure of the target tangential wind is specified by the empirical function $F(\sigma)$ of (4.1). Numerical values that seem appropriate for representing the vertical profile in the case of deep tropical cyclones are: 1.0, 0.97, 0.88, 0.82, 0.65, 0.35 for $\sigma = 0.85$, 0.7, 0.5, 0.4, 0.3, 0.2, respectively, and 0 above 0.15. Modification of the above values is needed when the storm depth is medium or shallow. (Values of 1.0, 0.95, 0.85, 0.5 for $\sigma = 0.85$, 0.7, 0.5, 0.4, respectively, and 0 above 0.3 has been tested for one case of a moderately deep system. For a shallow system, nontested values of 1.0, 0.9, 0.6 for $\sigma = 0.85$, 0.7, 0.5 and 0 above 0.4 are under consideration.) In the case in which upper-level wind observations are available, the vertical profile function will be used not to obtain the upper-level target wind but to determine the first-guess winds at upper levels from the target winds at the planetary boundary layer top (see appendix B).

c. *Time integration of the axisymmetric model (referred to in section 4a)*

The time integration of the axisymmetric model produces the symmetric vortex. In addition to the conditions mentioned in section 4a, the following are used in the model integration.

The radially and vertically varying parameter α of (4.3), when multiplied by the time step (20 s in the present study), represents a relaxation time of the tangential wind toward the reference value. Larger values of α imply weaker forcing. The form currently used to determine α is

$$\alpha(r, \sigma) = \max[\alpha_r(r), \alpha_\sigma(\sigma)]. \tag{6.5}$$

The values assigned are α_r (at 8, 15, 20, 25, 30, 35, 40, 56 radii in the unit of 1/6° latitude length) = 0, 5, 25, 50, 100, 200, 400, and 800, respectively, with linear variation between adjacent radii. Also, α_σ at any σ level is obtained by interpolation from α_σ(at 0.85, 0.7, 0.5, 0.4, 0.3, 0.2, 0.15) = 0, 40, 150, 300, 800, 1500, and ∞, respectively. The strongest forcing is imposed at low levels, where the target wind profile is presumed to be relatively reliable, and near the storm center. Relatively weak forcing at upper levels and outer regions allows less constrained flow evolution, for example, the appearance of anticyclonic winds at upper levels at large radii despite the cyclonic target wind. The above values of α should be modified when upper-level target winds become much more reliable, for example, through the incorporation of upper-level observations.

In general, the axisymmetric model is integrated to 60 h. The integration is terminated at an earlier time if the surface pressure difference between the radius r_b and the center exceeds $p_{out} - p_c + \delta p$. The additional factor δp, which allows for short-period intensity fluctuations, is set to the smaller value of 3 hPa and $a + b(p_{out} - p_c)$, where $a = 1$ hPa, $b = 0.04$, and $p_{out} - p_c$ is in hectopascals. If the pressure difference at 59 h is below this value, but a vortex of hurricane strength has evolved, the integration of the model is continued for one additional hour without tangential wind forcing. Any imbalance that may have developed in the model fields due to the forcing will be reduced during this period. For a vortex of weaker than hurricane strength at 59 h, the forcing is not eliminated during the additional 1-h period because storms in this case have tended to intensify once they are set free from the forcing constraint. This forcing is somewhat analogous to the forcing that is exerted by the environmental field and that frequently influences the intensification of tropical storms.

Finally, the treatment of the surface boundary conditions in the axisymmetric integration should be mentioned. The sea surface temperature is held fixed during the integration to the mean value for the 16

grid points (in 1° resolution) nearest to the storm center (λ_c, φ_c). If any of these points is a land point, it is excluded from the average. If the mean value is higher than 303 K, the mean of that value and 303 K is taken. For the axisymmetric integration, evapotranspiration is assumed to be at its maximum potential rate.

d. Computation of asymmetry (referred to in section 4b)

The asymmetric wind of the vortex is obtained from the time integration of the simplified vorticity equation. It takes one to two days for an initially symmetric vortex to develop a quasi-steady vortex drift. It is assumed that such a state is present in the case of mature tropical cyclones. However, for tropical cyclones in an early development stage, or for those undergoing rapid structural change, the asymmetric structure may not have developed quasi-steady drift, either because of a larger influence of the environmental flow or due to the large time variation of the symmetric flow. Thus, a reduction of the time-integration period for these cases seems to be a better approximation of a weaker or unsteady drift, although the above issue is still open for further investigation. In the present scheme, if the actual tropical cyclone 18 h earlier was weaker than tropical storm intensity, an 18-h integration period is used. If $p_{out} - p_c$ at 18 h earlier is less than one-half of $p_{out} - p_c$, rapid deepening is assumed, and the integration time is also set to 18 h. Otherwise, the integration is performed for 36 h.

7. Some results of automated implementation

The automated initialization method proposed in the present paper has been tested for eight cases: Hurricane Gloria, 1985, at a stage prior to its rapid intensification, at a stage of rapid intensification, and at a mature stage; Hurricane Gilbert, 1988; Hurricane Bob, 1991; Hurricane Fabian, 1991; Hurricane Grace, 1991; and Tropical Cyclone Connie, 1987. All of the above storms developed over the North Atlantic ocean, except Tropical Cyclone Connie which struck the northwest Australian coast. Table 1 lists the filter radius r_0 used to remove each of these storms from the large-scale analyses, as well as the radius r_b used in the generation of the symmetric structure of the specified vortices. The radius r_0 is always larger than r_b, except for Hur-

TABLE 1. Values of the filter radius, that is, the radius of the analyzed vortex r_0, and the radius of the specified vortex r_b for eight storms.

Storm (time)	r_0 (km)	r_b (km)
Gloria (1200 UTC 22 September 1985)	1097	745
Gloria (0000 UTC 24 September 1985)	1138	805
Gloria (0000 UTC 25 September 1985)	1194	960
Gilbert (1200 UTC 14 September 1988)	1333	1480
Bob (0000 UTC 18 August 1991)	917	805
Fabian (0000 UTC 28 October 1991)	917	664
Grace (0000 UTC 16 October 1991)	1291	1110
Connie (0000 UTC 18 January 1987)	1292	800

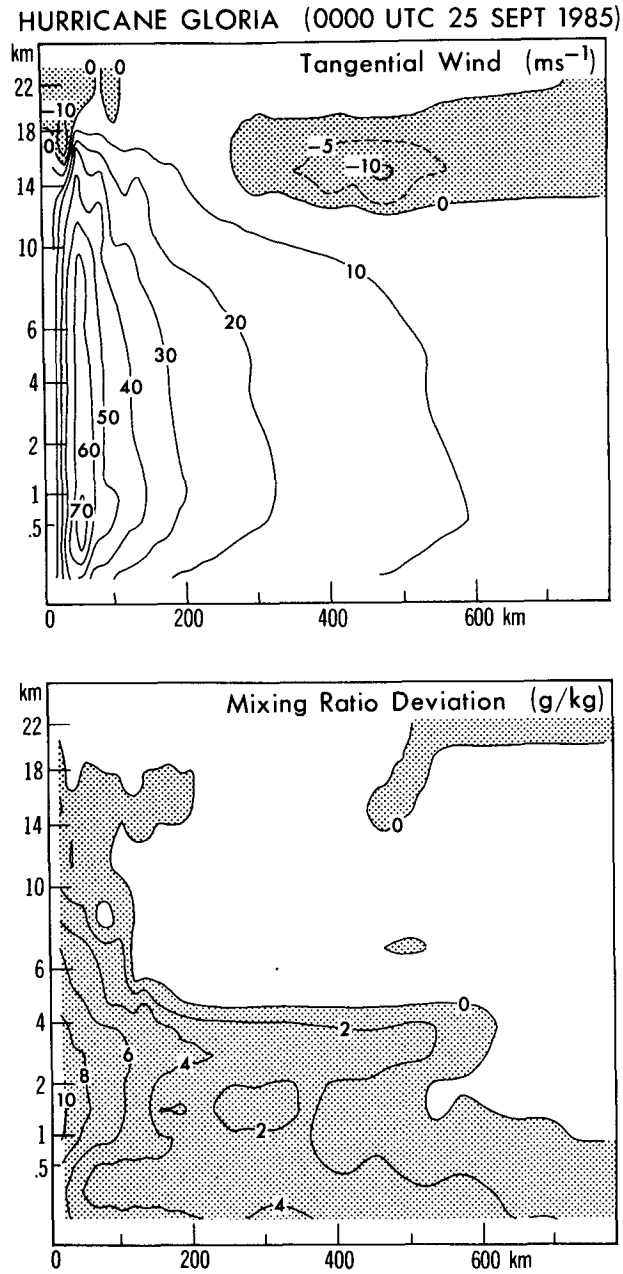

FIG. 3. Radius–height cross sections of the symmetric component of the model vortex generated by the time integration of the axisymmetric version of the GFDL hurricane model for Hurricane Gloria at 0000 UTC 25 September 1985. The tangential wind (m s^{-1}; anticyclonic flow shaded) and the deviation of the water vapor mixing ratio from that of the environmental state (g kg^{-1}; area with positive deviation shaded) are shown.

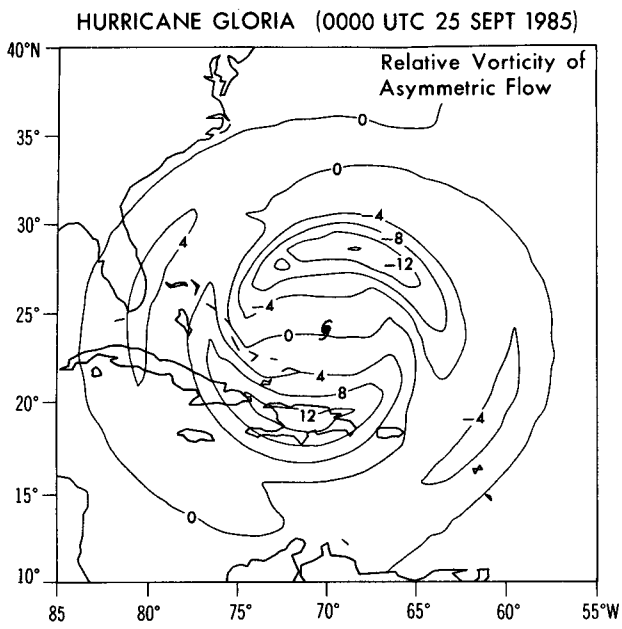

FIG. 4. Relative vorticity (10^{-6} s^{-1}) of the asymmetric flow generated for Hurricane Gloria at 0000 UTC 25 September 1985. Contour interval is 4×10^{-6} s^{-1}.

ricane Gilbert, and the two values are positively correlated for the Atlantic storms.

The proposed scheme produced initial hurricane fields that are more realistic than the global analyses. For example, in the case of Hurricane Gloria at the mature stage, 0000 UTC 25 September 1985, the central surface pressure in the model after the initialization is 913 hPa. This compares favorably with the observed values of 920 hPa. Figure 3 shows the radius–height cross sections of the tangential wind and the mixing ratio of water vapor (deviation) of the generated symmetric vortex. The wind field includes anticyclonic flow at upper levels. The radial flow (not shown) indicates the existence of an inflow layer below about 1 km and an upper outflow layer. Moisture excess in the vortex exceeds 2 g kg^{-1} over an area of about 500-km radius, with the maximum deviation of more than 10 g kg^{-1}. The asymmetry generation induced the field of relative vorticity shown in Fig. 4. It indicates that the dipolar (wavenumber 1) structure is the predominant part of the generated asymmetry, with a vorticity minimum (maximum) located approximately to the north (south) of the storm center. The boundary-layer top wind at the storm center, due to the above vorticity, is directed 62° west from due north with a speed of 2.87 m s^{-1}. The addition of the specified vortex, consisting of the symmetric and asymmetric component, to the environmental field yields the initial wind condition for the hurricane model. This field is compared against the field from the large-scale analysis in Fig. 5, in which the distributions of the wind speed on vertical cross sections taken along a latitude near the hurricane center are shown. The vortex produced by the proposed initialization method is much stronger and more compact.

Results of the experimental predictions using the present initialization scheme indicate quite encouraging performance of the GFDL triply nested movable mesh hurricane model in track prediction, especially in the early 48-h period. The mean forecast errors of positions at 12, 24, 36, 48, 60, and 72 h for the seven

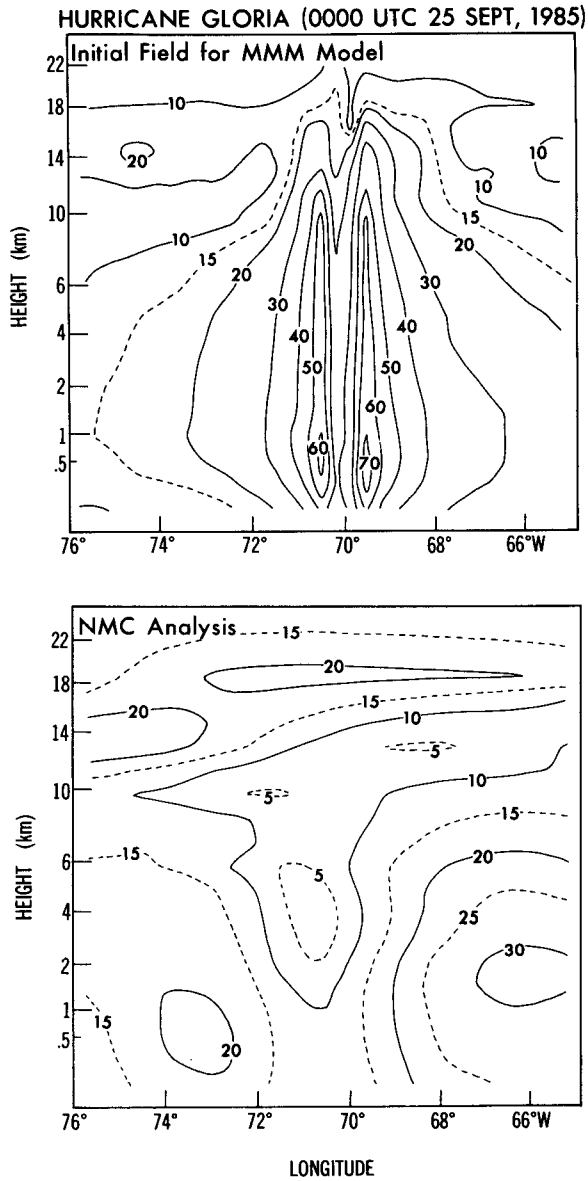

FIG. 5. Vertical cross sections of the wind speed (m s^{-1}) at 0000 UTC 25 September 1985. The section is taken along the latitude of the MMM model grid point, which is nearest to the center of Hurricane Gloria. The upper panel shows the distribution after the initialization with the vortex specification. The lower panel is for the same case but is taken from the NMC global analysis.

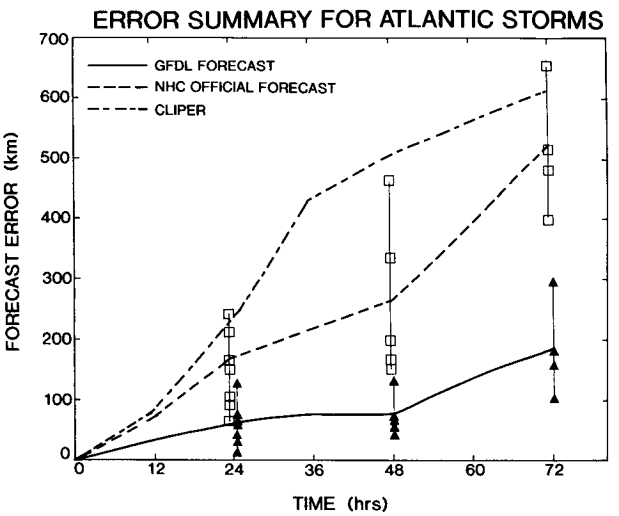

FIG. 6. Errors of tropical cyclone track predictions for seven cases of Atlantic storms. Average errors for the GFDL model forecasts (solid line), the official forecasts by NHC (dash line), and the CLIPER forecasts (dash–dot line) are compared. Errors at the 24-, 48-, and 72-h forecast for individual cases are shown by solid triangles for the GFDL forecasts and by open squares for official forecasts by NHC, respectively, which are plotted along thin vertical lines placed roughly at corresponding forecast times.

Atlantic storm cases listed in Table 1 are 35, 61, 77, 76, 137, and 183 km, respectively. These mean errors, along with individual cases, are compared in Fig. 6 against the average errors for the same cases from the official forecasts by the National Hurricane Center and the predictions with the CLIPER method, that is, the simple combination of climatology and persistence. A dramatic improvement in the track prediction using the present initialization scheme is clear for these cases. The reduction of forecast error in the initial 36–48 h is especially important to operational tropical cyclone forecast centers. The improvement at these earlier times results mainly from the satisfactory adaptation of the initial vortex to the prediction model, thus almost eliminating the adjustment process that leads to the erratic storm movement. As mentioned in Kurihara et al. (1990), the accurate prediction of the environmental field contributes to the improved track forecast in the later period. The experimental predictions also produced time changes of the storm intensity (not shown) that generally agree fairly well with the observed changes. This suggests that the past difficulty in predicting storm intensity, due to the false spinup of an initial vortex, has been greatly reduced by the proposed vortex specification. It should be stressed that an accurate intensity forecast requires an accurate track prediction, which leads to an accurate estimate of the interaction between the vortex and environmental fields as well as an accurate estimate of the air–sea interaction effects.

The model forecast improvement due to the present initialization scheme is examined in more depth in Bender et al. (1993). Specifically, predictions of track and intensity for the initialized and noninitialized forecasts of Hurricanes Gloria and Gilbert are compared. Presumably, further improvements in track and intensity prediction are possible with an increase in the number of wind observations used to define the target wind profile. For example, in the case of Tropical Cyclone Connie located to the northwest of Australia, the addition of four radiosonde observations to the wind dataset resulted in a reduction of the 72-h track prediction error from 371 to 249 km.

8. Summary and remarks

The automated initialization scheme of the GFDL hurricane prediction model is described in this paper. The basic strategy is to replace the poorly resolved vortex of a coarse-resolution analysis with a more realistic vortex that is constructed to better match the high-resolution hurricane prediction model.

Two spatial filters are used to remove the poorly resolved vortex from the large-scale analysis, leaving the environmental field. The specified vortex to be placed in the environmental field consists of a symmetric structure and an asymmetric flow. The symmetric component is generated from the time integration of the axisymmetric version of the hurricane prediction model, with an observationally derived constraint imposed on the tangential flow. The generated symmetric wind is used in the computation of the asymmetric component using a simplified barotropic vorticity equation. Thus, the latter component is consistent with the former. The mass field is then recomputed using a static initialization method in which the generated wind field is not modified.

The performance of the model using the initial conditions generated by the present scheme has been quite satisfactory in the cases tested so far. The success is attributable to the vortex specification method, which has been formulated so that the requirements set forth in section 2 are satisfied. Namely, this technique ensures the following desirable conditions: the smooth connection of the environmental field from the storm area to the surrounding domain; compatibility of the specified vortex to the resolution and physics of the prediction model; structural consistency of the generated vortex in the fields of wind, temperature, surface pressure, and moisture; and the incorporation of realistic features in the tangential flow of the vortex. The initialization method was designed to eliminate an initial adjustment and false spinup of the model vortex. As anticipated, the adaptation of the specified vortex to the hurricane prediction model has clearly shown a substantial improvement in the track prediction. In particular, the reduction of the forecasted track error

in the early period is largely due to the smooth movement of the specified vortex. Furthermore, encouraging forecast skill has been found in the prediction of intensity for most cases tested.

Both an improvement of the initialization scheme and an increase in the amount of accurate observational information will further refine the representation of tropical cyclones in the model initial conditions. For example, results from recent cases indicate that still further improvement in prediction may result from use of the tangential wind rather than the wind speed in the determination of the radius of the analyzed vortex, r_0. Also, as exemplified by the experimental prediction of Tropical Cyclone Connie, even a limited number of additional wind observations within 1000 km of the storm center will be quite useful. Thus, the need for enhanced wind observation should be emphasized. An extension of the initialization scheme to utilize upper-level wind observations and even a more comprehensive three-dimensional wind-field analysis (e.g., Lord and Franklin 1987) is a subject of future study. In such cases, the framework and technique described in the present paper will still be useful for generating the model-consistent initial conditions, for example, for generating the temperature and moisture fields for the given wind field by using a primitive equation model. Finally, the approach taken in this study of model initialization may be applicable to numerical models used for other mesoscale systems as well.

Acknowledgments. The authors express their thanks to their colleagues, in particular to Joseph Smagorinsky, Jerry Mahlman, Robert E. Tuleya, and Kikuro Miyakoda, who have given them constant encouragement and valuable advice during long-term development of this work. They are grateful to Robert E. Tuleya and Brian D. Gross for useful comments and suggestions for improvement of the original manuscript, and to reviewers, including Lloyd Shapiro, for valuable comments. They also thank Phil Tunison, Cathy Raphael, and Jeff Varanyak for preparing figures.

APPENDIX A

Definitions of Parameters and Functions

A, B	factors controlling the target tangential wind profile beyond r_a; see Eq. (6.3)
$E(r)$	cylindrical filtering function; see Eq. (3.8)
$F(\sigma)$	empirical function of the vertical profile of the target tangential wind
l	parameter controlling cylindrical filtering shape; see Eq. (3.8)
p_c	central pressure of the observed vortex
p_{out}	pressure of the last closed isobar
r_0	radius of the analyzed vortex
r_a	radial location of the outermost observation point
r_b	radius of the specified vortex
r_f	preliminary estimate of cylindrical filter size
r_{out}	radius of the last closed isobar
R_{DM}	radius of maximum V_D
$R_{\max}$	radius of maximum wind
$\langle V \rangle$	target tangential wind in the free atmosphere; see Eq. (4.1)
$\langle V_d \rangle$	radial profile of the target tangential wind at the boundary-layer top
V_D	wind speed of the disturbance field at the boundary-layer top
$\overline{V_D}$	circular mean of V_D at any radius
$V_{\max}$	maximum surface wind speed
V_{obs}	observed tangential wind data used to define $\langle V_d \rangle$
V_R	time-dependent reference wind determined from the target wind, $\langle V \rangle$
α	weighting parameter for the reference wind forcing; see Eqs. (4.3), (6.5)
α_r, α_σ	radial and vertical variation of weighting parameter α; see Eq. (6.5)
λ_c, φ_c	longitude, latitude position of the observed vortex
λ_0, φ_0	longitude, latitude position of the analyzed vortex; see Eq. (6.1)
τ	long time scale used to determine the reference wind, V_R; see Eq. (4.2)

APPENDIX B

Target Winds in the Free Atmosphere

As mentioned in sections 4a and 6b, the hurricane message and observational data currently available in practice are only for the low-level winds. In such a case, this information is used separately for each of the four quadrants to modify a first-guess wind profile that is applicable to the top of the planetary boundary layer. The four profiles obtained are then averaged to define the target tangential wind profile at the planetary boundary-layer top. As shown by (4.1), the target tangential wind in the free atmosphere is determined by using the functional representation of the vertical profile of the tangential wind.

In the above process, and in the following as well, the observed data in each of the four quadrants are arranged according to the observed position by taking only the radial distance from the storm center into account. If more than one observation exists in an appropriately divided small radial interval, the group should be represented as one "super observation" whose value and radial position are simply the averages taken for the data group. This will suppress unrealistically large radial variation of data, which may otherwise result from data sampling problems.

If some sporadic upper-level wind data such as the Omega dropwindsonde observations are available, the

present scheme may be modified as follows to utilize this data for improving the estimate of the target tangential wind in the free atmosphere. Specifically, after the modified wind profiles at the boundary-layer top are obtained for the four quadrants, each one is multiplied by the vertical profile function of (4.1) to define first-guess wind profiles at upper levels in the respective quadrant. These new first-guess wind profiles are then modified by incorporating the available observations by the same procedure as used for the observed data at the boundary-layer top. Finally, the four modified profiles at each level are averaged to define the target tangential wind profile for that level.

In the case where the available wind information is dense enough to make a comprehensive three-dimensional wind analysis (e.g., Lord and Franklin 1987) of a tropical cyclone, the analyzed field may be regarded as the target wind field. A model-consistent initial vortex may possibly be generated from the time integration of a full hurricane model with the wind fields appropriately forced to the target state. A study along this line is planned.

REFERENCES

Akima, H., 1970: A new method of interpolation and smooth curve fitting based on local procedures. *J. Assoc. Computing Machinery,* **17,** 589–602.

Bender, M. A., and Y. Kurihara, 1987: A numerical study of the effect of the mountainous terrain of Japan on tropical cyclones. *Short- and Medium-Range Numerical Weather Prediction,* T. Matsuno, Ed., Meteorological Society of Japan, 651–663.

——, R. J. Ross, R. E. Tuleya, and Y. Kurihara, 1993: Improvements in tropical cyclone track and intensity forecasts using the GFDL initialization system. *Mon. Wea. Rev.,* **121,** 2046–2061.

Carr, L. E., and R. L. Elsberry, 1990: Observational evidence for predictions of tropical cyclone propagation relative to environmental steering. *J. Atmos. Sci.,* **47,** 542–546.

——, and ——, 1992: Analytical tropical cyclone asymmetric circulation for barotropic model initial conditions. *Mon. Wea. Rev.,* **120,** 644–652.

Depperman, C. E., 1947: Notes on the origin and structure of Philippine typhoons. *Bull. Amer. Meteor. Soc.,* **28,** 399–404.

Holland, G. J., 1980: An analytic model of the wind and pressure profiles in hurricanes. *Mon. Wea. Rev.,* **108,** 1212–1218.

Iwasaki, T., H. Nakano, and M. Sugi, 1987: The performance of a typhoon track prediction model with cumulus parameterization. *J. Meteor. Soc. Japan,* **65,** 555–570.

Kurihara, Y., M. A. Bender, R. E. Tuleya, and R. J. Ross, 1990: Prediction experiments of Hurricane Gloria (1985) using a multiply nested movable mesh model. *Mon. Wea. Rev.,* **118,** 2185–2198.

Lord, S. J., and J. L. Franklin, 1987: The environment of Hurricane Debby (1982). Part I: Winds. *Mon. Wea. Rev.,* **115,** 2760–2780.

Mathur, M. B., 1991: The National Meteorological Center's quasi-Lagrangian model for hurricane prediction. *Mon. Wea. Rev.,* **119,** 1419–1447.

Neumann, C. J., 1979: On the use of deep-layer-mean geopotential height fields in statistical prediction of tropical cyclone motion. *Proc. Sixth Conf. on Probability and Statistics in Atmospheric Sciences,* Banff, Amer. Meteor. Soc., 32–38.

Reeder, M. J., R. K. Smith, and S. J. Lord, 1991: The detection of flow asymmetries in the tropical cyclone environment. *Mon. Wea. Rev.,* **119,** 848–854.

Ross, R. J., and Y. Kurihara, 1992: A simplified scheme to simulate asymmetries due to the beta effect in barotropic vortices. *J. Atmos. Sci.,* **49,** 1620–1628.

Smith, R. K., W. Ulrich, and G. Dietachmayer, 1990: A numerical study of tropical cyclone motion using a barotropic model. Part 1. The role of vortex asymmetries. *Quart. J. Roy. Meteor. Soc.,* **116,** 337–362.